Indian Journal of Chemical Technology
Vol. 32, January 2025, pp. 125-136
DOI: 10.56042/ijct.v32i1.14810

Chitosan-alginate complex for the controlled delivery of α-lipoic acid in diabetes therapy: Modulation by montmorillonite and glutaraldehyde

Dikshita Sharma[1], Atifa Sarkar[1], Archana Sinha[2], Suman Dasgupta[2] & Tarun K. Maji[1]*

[1] Department of Chemical Sciences & [2]Department of Molecular Biology and Biotechnology, Tezpur University, Napaam, Sonitpur, Assam-784 028, India

*E-mail: tkm@tezu.ernet.in

Received 3 November 2024; accepted 26 December 2024

Development of safe, therapeutically effective, and patient-compliant drug delivery systems remains a key focus in pharmaceutical research, particularly for controlled-release formulations. In this study, Lipoic acid-loaded chitosan-alginate polyelectrolyte complexes have been successfully prepared, incorporating varying concentrations of Montmorillonite (MMT) nano clay as a filler and glutaraldehyde (GA) as a crosslinking agent. The effects of varying GA and MMT concentrations on drug loading and encapsulation efficiency are investigated in detail. The structural characteristics of the complexes are analysed using Fourier Transform Infrared Spectroscopy (FTIR), X-ray Diffraction (XRD), and Scanning Electron Microscopy (SEM). The *in vitro* drug release is studied over 50 h using a UV-visible spectrophotometer at two pH levels (1.2 and 7.4), demonstrating that the cumulative release of Lipoic acid is pH-dependent. Additionally, cumulative drug release decreases with increasing concentrations of GA and MMT, likely due to increased crosslinking density and restricted swelling of the complex. Glucose uptake assays show significant improvement across all formulations, and MTT assays confirmed that the drug formulations are non-toxic, maintaining cell viability. Overall, these results suggest that the lipoic acid-loaded chitosan-alginate polyelectrolyte complexes are promising candidates for future development in treating insulin resistance and type 2 diabetes, with the potential to enhance therapeutic efficacy through controlled drug release.

Keywords: Biopolymer, Chitosan-alginate complex, Drug delivery, Sustained hypoglycaemia, Targeted drug delivery

Introduction

Diabetes mellitus is a chronic metabolic disorder characterised by elevated blood glucose levels, which can lead to various complications such as cardiovascular disease, neuropathy, and nephropathy[1]. Diabetes affects millions of people worldwide, with a particularly high prevalence in middle- and low-income countries[2]. Effective management and treatment options for diabetes are paramount. Natural bioactive compounds, such as α-lipoic acid (LA), have gained significant attention in diabetes management due to benefits like biocompatibility, safety, synergistic effect, low cost and multitherapeutic action. LA is a naturally occurring compound that plays a vital role in cellular energy metabolism. It functions as a coenzyme in various biochemical reactions, particularly in the metabolism of carbohydrates, making it potentially relevant for managing diabetes and its associated complications. LA has been shown to enhance insulin sensitivity[3-5]. It enhances glucose absorption by stimulating insulin signalling pathways, which results in a more significant movement of glucose transporter type 4 (GLUT4) to the cell surface. This mechanism aids in entering glucose into cells, lowering insulin resistance and enhancing blood sugar management[6]. A computer modelling study indicated that lipoic acid could attach to the intracellular tyrosine kinase domain of the insulin receptor and help maintain the enzyme's active form[7]. Studies suggest that LA supplementation can enhance mitochondrial function and energy metabolism, particularly in those with metabolic disorders. Additionally, LA offers neuroprotective benefits, especially in treating diabetic neuropathy. It has been found to improve nerve conduction and alleviate neuropathy symptoms, including pain and tingling in the extremities[8]. On the contrary, LA is reported to have compromised stability in the gastric environment, low bioavailability and a brief half-life, requiring multiple doses and resulting in variable therapeutic levels[9]. A controlled-release drug delivery system utilising biopolymers tackles these challenges by offering a prolonged release, boosting stability and bioavailability, minimising side effects, and enhancing patient adherence.

Biopolymers, such as chitosan and alginate, have garnered significant interest in drug delivery systems due to their inherent biocompatibility, biodegradability, and pH-responsive properties[10,11]. Chitosan, derived from chitin, displays exceptional properties, including gel-forming behaviour in response to low pH conditions, such as those encountered in the stomach. This unique property protects the drug during gastric transit and controlled release at the target site, maximising therapeutic efficacy.[12,13] Additionally, it can be easily decomposed by enzymes like chitinase and lysozyme found in the human body. This enables chitosan-based substances to break down into non-harmful byproducts, reducing the likelihood of buildup in tissues. The degradation rate can be adjusted by altering the degree of deacetylation or by combining chitosan with other polymers, making it useful for controlled drug delivery applications[14,15].

Alginate, a biopolymer derived from brown seaweed, further optimises the drug delivery system. It offers remarkable gel-forming capabilities, imparting mechanical strength and stability to the system. Additionally, alginate undergoes ionisation and gelation in the presence of calcium ions, further enhancing its pH-responsive behaviour[16]. The impressive gel-forming properties are mainly due to its capacity to create hydrogels when divalent cations like calcium ions (Ca^{2+}) are present. This gelation mechanism includes ionic cross-linking, which improves the drug delivery system's mechanical strength and stability[17,18]. Alginate is composed of units of mannuronic acid (M) and guluronic acid (G). The G-blocks play a vital role in gel formation because they interact with calcium ions to form a stable network structure called the "egg-box" model[18,19]. This configuration provides considerable mechanical strength, enabling alginate hydrogels to endure mechanical stress, which is advantageous for various biomedical uses[20]. Alginate also demonstrates pH-responsive characteristics due to the ionisation of its carboxylic acid groups. Alginate tends to contract in acidic conditions, while in alkaline environments; it expands because of electrostatic repulsion between negatively charged chains[21]. This attribute is particularly useful for targeted drug delivery, as it facilitates controlled release in response to specific physiological conditions[21,22].

Combining chitosan and alginate as biopolymeric polyelectrolyte complexes provides precise control over drug release, improving therapeutic outcomes and minimising potential side effects. By adjusting the mass ratio of sodium alginate to carboxymethyl chitosan, the system can achieve high swelling rates in both acidic and alkaline environments, allowing for targeted drug release. Drug release studies indicate that a 1:3 mass ratio promotes gastric release, while a 3:1 ratio favours release in the intestines[23]. In this work, we focus primarily on intestine-targeted controlled delivery, as intestinal release is preferred over gastric release for the oral delivery of LA. This preference stems from its greater instability in acidic environments and better absorption in the small intestine. This approach also reduces gastric irritation and enhances the drug's bioavailability[9].

Crosslinkers are incorporated into the polymer matrices to enhance further the mechanical integrity and controlled drug release dynamics of chitosan and alginate polymers. A synergistic approach between physical and chemical crosslinkers is helpful in drug delivery. Physical crosslinkers like calcium chloride induce ionic crosslinking, which is typically reversible and suitable for softer dynamic systems. Chemical crosslinkers, like glutaraldehyde, induce covalent crosslinking, leading to stronger, permanent, and more stable materials. Glutaraldehyde crosslinking enhances the mechanical strength of chitosan hydrogels, improving properties like storage modulus and yield stress[24]. Additionally, in alginate-based materials, glutaraldehyde (GA) crosslinking enhances mechanical properties, with the highest tensile strength observed at 5% GA concentration[25]. Furthermore, chitosan films with GA exhibit improved tensile resistance and reduced water vapour permeability, making them competitive for packaging applications[26]. The crosslinking of chitosan films with glutaraldehyde also affects their biodegradability, showing that while crosslinking does not prevent degradability, it prolongs the process[27].

In our research, we investigated the effect of varying the concentration of the crosslinker and filler in the pH-responsive drug delivery system. Including montmorillonite (MMT) nano clay as a filler facilitates controlled release mechanisms crucial for maintaining therapeutic levels over extended periods. The intercalation of drugs within the clay layers allows for a gradual release, reducing dosing frequency and improving patient compliance[28,29]. Incorporating MMT into polymer matrices enhances the mechanical properties of drug delivery systems,

contributing to their stability and durability[30]. MMT is known for its excellent biocompatibility and low toxicity, making it suitable for medical applications. Its natural origin and non-toxic nature reduce the risk of adverse reactions, ensuring patient safety in long-term therapies[31,32]. By systematically altering the concentrations of the crosslinker and filler, we aimed to assess their impact on drug release kinetics, stability, and overall system performance.

The design of a pH-responsive controlled release system offers significant potential for optimising oral drug delivery for antidiabetic therapy. This study presents the development of a novel pH-responsive drug delivery system for the oral administration of LA, a potent antidiabetic agent. We employ biopolymers, specifically chitosan and alginate, in conjunction with glutaraldehyde as a crosslinker and Montmorillonite (MMT) nano-clay as filler. Additionally, we thoroughly investigate the impact of varying concentrations of both the crosslinker and the filler on the performance of this drug delivery system.

Experimental Section

Materials

Chitosan was purchased from Sigma Alrich, USA. Sodium alginate, α-lipoic acid (LA) (extra pure), and calcium chloride dihydrate were purchased from Sisco Research Laboratory, India. Sigma Aldrich, USA, supplied montmorillonite nano-clay. Glutaraldehyde was purchased from Loba Chemi Pvt. Ltd. Mumbai, India. Tween80 and Ethanol were procured from E-Merck, India. The rest of the chemicals were of analytical grade and used as such.

Methods

Preparation of Glutaraldehyde crosslinked Lipoic acid loaded Chitosan-MMT-Alginate polyelectrolyte complex (PEC)

The chitosan-alginate complex was synthesised following a previously reported protocol with slight modifications[32-34]. Sodium alginate solution, 0.3% (w/v), was prepared by dissolving sodium alginate in water, and the pH was adjusted to 5.1 by adding HCl dropwise while maintaining constant stirring at room temperature. A 20% (w/v) solution of calcium chloride ($CaCl_2$) in water was added dropwise to induce crosslinking of the alginate. A known amount of MMT (0-0.06 g) pre-dispersed in water by constant stirring for 24 h followed by sonication, was added to the alginate under continuous stirring. Tween 80 was added to the mixture to ensure uniform dispersion. Separately, LA (0.01 g) dissolved in a 1:1 ethanol-water solution was added very slowly to the sodium alginate-MMT solution, and constant stirring was maintained for 2-3 h. A known amount of 0.1% (w/v) chitosan solution, prepared in 1% (v/v) acetic acid with the pH adjusted to 5.4, was gradually incorporated into the sodium alginate solution, and stirring was continued for 30 min. The temperature was then lowered to 0-5°C. At this point, GA (0-15 µL) was added dropwise to the mixture, and the temperature was raised to 45°C. Stirring was maintained for 3-4 h to facilitate cross-linking. The resulting suspension was allowed to cool to room temperature and centrifuged. The product was freeze-dried to obtain the product. A series of samples were prepared by varying the concentrations of crosslinker and nano-clay.

Calculation of process yield

The process yield was determined using the following equation[35].

$$Process\ \ yield(\%) = \frac{Weight\ of\ the\ product}{Weight\ of (Drug + MMT + Polymer)} \times 100 \quad \ldots (1)$$

Calibration curve of Lipoic acid

A calibration curve is essential for determining the drug's loading, encapsulation efficiency, and release rate from the complex within an appropriate solvent medium (ethanol-water), and it is plotted following the established protocol.[36]

A series of known concentrations of LA (prepared in double-distilled water) were analysed using a UV-visible spectrophotometer (UV-2001, Hitachi, Tokyo, Japan) across the 200–600 nm wavelength range. A characteristic absorbance peak was observed between 227 and 334 nm, corresponding to LA concentrations ranging from 0.001 to 0.005 g per 100 mL.

The absorbance values at 227–334 nm for each concentration were recorded and plotted, generating a calibration curve showing a linear relationship between absorbance and concentration. This calibration curve was subsequently used to estimate the unknown concentrations of LA in release studies based on the measured absorbance values at the corresponding wavelength.

Calculation of encapsulation efficiency and drug loading efficiency of the polyelectrolyte complex

After ultracentrifuging the samples at room temperature for 30 min, the drug loading efficiency (LE) and encapsulation efficiency (EE) from different

formulations were assessed. The concentration of unencapsulated LA in the supernatant was determined by measuring its absorbance at wavelengths between 227 and 334 nm using a UV-visible spectrophotometer. The calibration curve is shown in Fig. 1. The EE value was then calculated using a standard formula, as outlined in the relevant literature[33].

$$Loading\ efficiency(LE)\% = \frac{(Total\ amount\ of Drug - Free\ amount\ of drug)}{Total\ amount\ of\ drug} \times 100 \quad \ldots (2)$$

$$Encapsulation\ efficiency(EE)\% = \frac{(Total\ amount\ of Drug - Free\ amount\ of\ drug)}{Weight\ of\ dry\ polyectrolyte\ complex} \times 100 \quad \ldots (3)$$

In vitro drug release studies

Dried samples containing lipoic acid-loaded complexes were weighed and immersed in phosphate buffer solutions at pH 1.2 and 7.4 to simulate gastric and intestinal pH, respectively. The samples were continuously stirred in these solutions to simulate drug release under physiological conditions. At predetermined time intervals, 5 mL of the solution was withdrawn, filtered, and analysed spectrophotometrically at 227–334 nm using a UV-visible spectrophotometer to measure the cumulative drug release at each time point. An equal amount (5 mL) of fresh buffer solution at the corresponding pH was added to the beaker to maintain a constant volume. This process was repeated three times for each determination to ensure reproducibility[37,38].

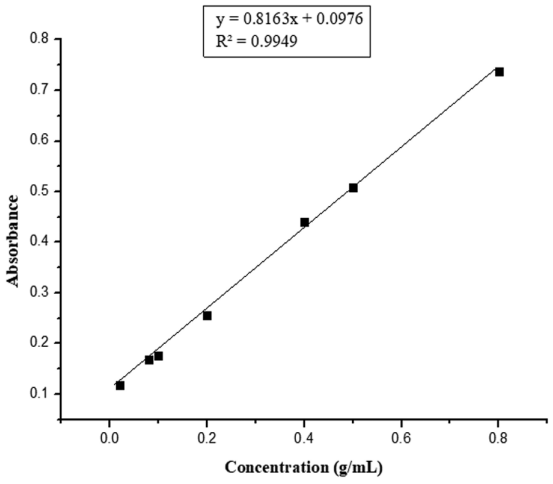

Fig. 1 — Calibration curve of Lipoic Acid

Characterisation

Fourier Transform Infrared Spectroscopy Study

A spectrophotometer model Impact-410 by Nicholet was used to record the Fourier transform infrared (FTIR) spectra in the range of 4,000–400 cm^{-1}, with a KBr pellet. Na-alginate, chitosan, LA, MMT, lipoic acid-loaded chitosan-alginate PEC, GA crosslinked lipoic acid-loaded chitosan-alginate PEC, and lipoic acid-loaded chitosan-MMT-alginate PEC were each finely grounded with KBr separately and prepared for the spectroscopy study.

X-ray diffraction study

X-ray diffractograms of LA, LA-loaded chitosan-alginate complex, GA-crosslinked-LA-loaded chitosan-alginate complex, LA-loaded chitosan-MMT-alginate complex, and GA-crosslinked-LA-loaded-chitosan-MMT-alginate complex were recorded on an X-ray diffractometer to determine the crystallinity distribution of Lipoic acid and the intercalation in the polymer complex. A Rigaku X-ray diffractometer (Miniflax, UK) was used to scan the samples from $2\theta=10^{o}$ to 80^{o}, with a scanning rate of 1^{o}/min, using Cu Kα (λ=0.15nm) radiation.

Scanning electron microscope study

Surface morphology can be studied using scanning electron microscopy. The scanning electron microscope (Model-JEOL ISM-6390 LV) used samples deposited on a brass holder sputtered with platinum. The surface morphologies of the samples were studied at an accelerated voltage of 20 kV.

Glucose Uptake Assay

The glucose uptake assay used a cell-based assay kit (Cayman, USA) and followed a previously documented method[39]. L6 myotubes were starved of serum overnight in Kreb's Ringer Phosphate (KRP) buffer with 0.2% bovine serum albumin (BSA). Cells were treated with KRP buffer alone, taken as a control set and served as a baseline to assess normal glucose uptake without any experimental manipulation.The cells were then treated with LA-loaded Chitosan-Alginate PEC having varied crosslinker (GA) and MMT concentrations (100 µg/mL) for 1 h. Cells were exposed to 0.75 mM palmitic acid for 6.5 h to induce a state mimicking insulin resistance, a common pathological condition in type 2 diabetes. This group evaluates the formulations' ability to counteract lipid-induced impairments in glucose uptake. Insulin (100 nM) was administered before concluding the incubations. 2-NBDG, a fluorescently labelled glucose analogue, was added 5 min before ending the

experiment in each incubator. Subsequently, the cells were lysed, and the fluorescent intensity was measured using the Varioskan LUX Multimode Microplate Reader (Thermo Scientific, Finland). Each sample was tested in triplicate.

Cell Viability Assay

Cell viability was determined using the MTT assay, following a previously described protocol[40,41]. Differentiated THP-1 macrophages were seeded in 96-well plates and exposed to various concentrations of the drug formulation for 24 h. After treatment, 10 µL of MTT reagent (5 mg/mL in PBS) was added to each well and incubated for 4 h at 37°C. The resulting formazan crystals were dissolved in 100 µL of acidic isopropanol and further incubated for 30 min at 37°C. Cytotoxicity was assessed by measuring absorbance for each sample in three different concentrations (20 µg/µL, 40 µg/µL, 100 µg/µL) at 570 nm using a Multiskan GO Microplate spectrophotometer (Thermo Scientific, Finland). Absorbance values were blanked against wells containing only acidic isopropanol, and untreated cells (exposed to medium only) were used as the control, representing 100% cell viability. Each assessment was performed in triplicate.

Statistical Analysis

The data underwent statistical analysis using one-way analysis of variance (ANOVA), with $p < 0.05$ considered statistically significant and expressed as means ± standard deviation (SD). Error bars in graphs indicate the standard deviation from three independent experiments.

Results and Discussion

Process yields, Drug encapsulation efficiency, and Drug loading efficiency

The process yield was calculated using the formula provided in Eq. (1). Table 1 shows the yield, encapsulation efficiency, and drug loading efficiency results for various polymer systems developed for delivering LA, illustrating the impact of varying MMT and GA concentrations on the properties of Ch/Alg complex. Variation in MMT concentration did not produce much impact on yield (%), which was found to decrease with an increase in crosslinker concentration. This might be due to loss during isolation. Complexes crosslinked without MMT demonstrated higher encapsulation and drug loading efficiency than those with MMT. As the MMT content increased, the encapsulation efficiency and drug loading efficiency decreased. This effect can be attributed to the interaction between the –OH groups of MMT's silicate layers, the –OH and $–NH_2$ groups in chitosan and the –COOH groups of alginate, causing the extension of the polymer chains to extend. The silicate layers in MMT restrict the free movement of intercalated polymer chains, forming a porous structure during dehydration, with multiple small channels running from the interior to the outer surface of the complex. As a result, part of the drug could diffuse out of the complex into the surrounding medium, lowering both encapsulation efficiency and drug loading efficiency[42,43]. The absence of MMT layers in the MMT-free crosslinked complex eliminated the hindrance observed in those with MMT. Additionally, incorporating MMT may reduce the available space for drug accommodation, leading

Table 1 — Effect of GA and MMT on properties of LA loaded Chitosan-Alginate complex[$]

Sample Code[#]	Chitosan % w/v (amount in g in 50 mL water)	Alginate % w/v (amount in g in 50 mL water)	Amount of crosslinker, % v/w (in µL)	Amount of MMT clay, % w/w w.r.t. CA (g in 50 mL water)	Process yield (%)	Encapsulation efficiency (%)	Drug loading efficiency (%)
CA	0.1 (0.05)	0.3 (0.15)	0	0	70.4(±0.03)	64.2(±0.04)	49.3(±0.01)
CA/GA1	0.1 (0.05)	0.3 (0.15)	2.5 (5)	0	68.2(±0.03)	61.9(±0.02)	46.8(±0.03)
CA/GA2	0.1 (0.05)	0.3 (0.15)	5 (10)	0	69.7(±0.02)	60.4(±0.05)	42.9(±0.05)
CA/GA3	0.1 (0.05)	0.3 (0.15)	7.5 (15)	0	67.1(±0.03)	57.8(±0.02)	38.2(±0.05)
CA/M1	0.1 (0.05)	0.3 (0.15)	0	0.3 (0.015)	70.8(±0.02)	62.8(±0.05)	40.6(±0.04)
CA/M2	0.1 (0.05)	0.3 (0.15)	0	1.2 (0.06)	71.4(±0.01)	60.2(±0.04)	38.2(±0.01)
CA/M3	0.1 (0.05)	0.3 (0.15)	0	4.8 (0.24)	71(±0.02)	61.4(±0.03)	38.9(±0.04)
CA/GA2/M2	0.1 (0.05)	0.3 (0.15)	5 (10)	1.2 (0.06)	68.46(±0.02)	55.2 (±0.01)	34.5(±0.02)

Lipoic Acid = 0.01 g, Tween 80 = 0.015 mL.
[#]In the sample code, Chitosan-Alginate PEC, glutaraldehyde, and MMT are represented by "CA," "GA," and "M," respectively.
[$]Each value and the standard deviation in parentheses represent the average of five readings.

to a decline in encapsulation and loading efficiency. Similarly, as the concentration of crosslinker GA increased, the encapsulation efficiency of the complex decreased. GA might restrict the free movement of polymer chains, promoting the formation of a porous structure. The drug could migrate through these pores or channels from the complex's interior to the surrounding medium. Moreover, interactions with the crosslinker may cause the polymer to become more rigid and compact, reducing the internal free volume. Consequently, encapsulation and drug loading efficiency both diminished. As per expectation, the combined effect of both MMT and GA decreased the encapsulation and drug loading efficiency.

In vitro release studies

The drug release study for the complex was conducted at two different pH levels, 1.2 and 7.4, over 1 to 50 h, as shown in Fig. 2. The cumulative release (%) of LA from the complex was found to be dependent on pH. Drug release was higher in the alkaline medium compared to the acidic medium. In an acidic medium, the amino groups of chitosan became protonated, thereby enhancing interaction with the carboxylate groups of Na-Alg to form a compact structure. Hence, the rate of swelling and the rate of release of LA would decrease. Further, LA's protection was likely also due to the stronger retention by the tightly bound alginate network that forms at low pH in the acidic environment. In contrast, in the alkaline medium, the deprotonation of chitosan decreased the interaction between chitosan and Na-Alg, thus facilitating the swelling to occur more. This would accelerate the release of LA. Additionally, in the alkaline medium, the breakdown of hydrogen bonding between the polymer and LA promoted drug release, resulting in higher cumulative release. The significant swelling of the complex at alkaline pH allowed easier solvent access to the drug within the polymer matrix, enhancing contact and thus enabling higher drug release[44,45].

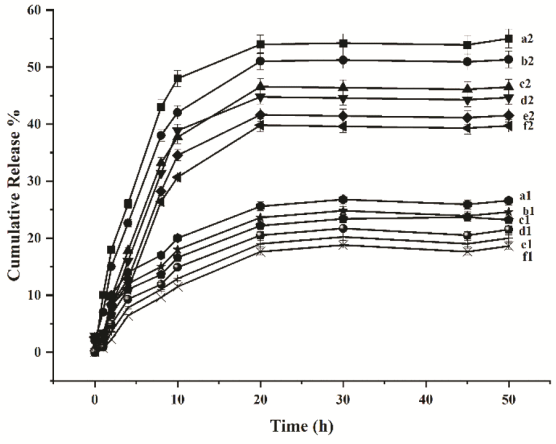

Fig. 2 — Effect of variation of concentration of GA and MMT on the percentage cumulative release of LA from drug-loaded complex at pH 7.4 {(a2) CA, (b2) CA/M1, (c2) CA/M3, (d2) CA/GA1, (e2) CA/GA3, (f2) CA/GA2/M2}, and pH 1.2 {(a1) CA, (b1) CA/M1, (c1) CA/M3, (d1) CA/GA1, (e1) CA/GA3, (f1) CA/GA2/M2}

The data indicated that LA's cumulative release (%) decreased as the MMT content and time increased. The silicate layers of MMT acted as a barrier for the solvent molecules to enter the complex. The higher the concentration of MMT, the higher was the resistance. Consequently, the ability of solvent particles to reach the LA molecules encapsulated in the complex became restricted, and thus, it decreased. The drug release increased up to a specific time and then remained almost unchanged throughout the time period. With time, the swelling of the complex increases, allowing more solvent particles to reach the drug molecule and assist in the release of LA from the complex[43]. The data indicated that LA's cumulative release(%) decreased as the concentration of GA increased. This was attributed to the higher crosslinking density of the complex at higher GA concentrations. Increased GA concentration produces a more crosslinked complex, reducing solvent access to the LA molecule encapsulated in the polymer complex and decreasing its release[46]. Therefore, there is a decrease in the cumulative release of LA.

Characterisation

Fourier transform infrared spectroscopy

In the FTIR spectra (Fig. 3A), curve (a) corresponds to the spectrum of sodium alginate. Key peaks include a broad band at 3452 cm^{-1}, attributed to O-H stretching, indicative of the hydroxyl groups in the polysaccharide structure. The band at 1603 cm^{-1} is associated with C=O stretching from the carboxylate groups of alginate, while the peak at 2920 cm^{-1} corresponds to C-H stretching. The band observed at 1396 cm^{-1} is due to COO^- stretching, and a strong band at 1021 cm^{-1} is linked to C-C and -OOC bond vibrations. A peak at 816 cm^{-1} is also assigned to Na–O bonding, a characteristic feature of sodium alginate.[47]

Curve (b) shows the spectrum of LA. A broad absorption band around 3460 cm^{-1} is assigned to O–H stretching. Peaks at 1691 cm^{-1} and 929 cm^{-1} are attributed to C–O stretching and out-of-plane O–H

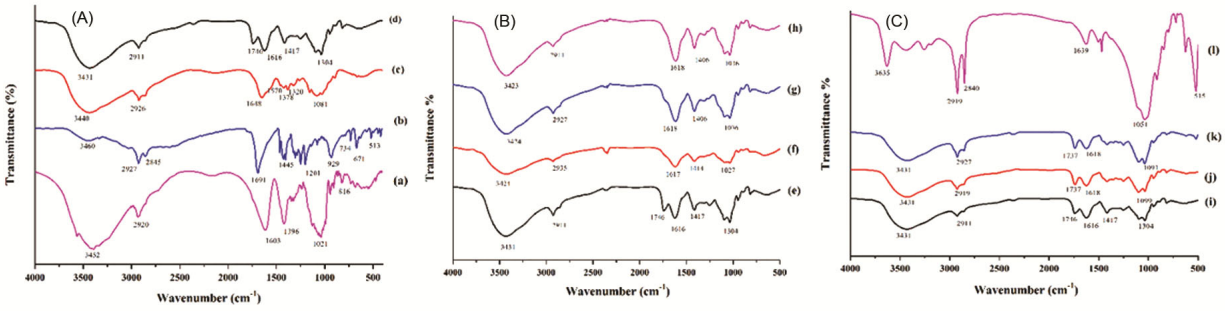

Fig 3. — FTIR spectra of (a)Alginate, (b) Lipoic Acid, (c) Chitosan, (d) CA, (e) CA, (f) CA/GA1, (g) CA/GA3, (h) CA/GA2/M2, (i) CA (j) CA/M1, (k) CA/M3 and (l) MMT (i) CA (j) CA/M1, (k) CA/M3, (l) MMT

bending of the carboxylic acid group. The region between 2927–2845 cm^{-1} displays weaker absorption due to overlapping C–H and O–H stretching bands. Peaks at 1445 cm^{-1} and 734 cm^{-1} are associated with CH_2 scissoring and rocking vibrations, while the region between 1445–1201 cm^{-1} is linked to a combination of C–O stretching, O–H bending, and CH_2 twisting. Additionally, peaks at 671 cm^{-1} and 513 cm^{-1} correspond to C–S and S–S stretching vibrations.[48]

Curve (c) represents the FTIR spectrum of chitosan. The O-H stretching band is located at 3440 cm^{-1}, while a peak at around 1648 cm^{-1} is due to the amide I band, indicative of the C=O stretching in chitosan's structure. A peak at 1570 cm^{-1} corresponds to N-H bending, confirming the presence of amino groups. The band at 2926 cm^{-1} is associated with C-H stretching. The peaks around 1378 cm^{-1} and 1320 cm^{-1} are linked to CH_2 bending and amide III bands, respectively, and the peak at 101 cm^{-1} corresponds to the C-O-C stretching vibration, characteristic of the glycosidic linkages in chitosan.

Curve (d) represents the FTIR spectrum of the LA-loaded chitosan-alginate complex. Several significant changes can be observed in this spectrum compared to the individual spectra of sodium alginate, chitosan, and lipoic acid. The OH stretching band shifted from 3452 cm^{-1} in Na-alginate and 3440 cm^{-1} in chitosan to 3431 cm^{-1}, indicating hydrogen bond formation between the OH and NH_2 groups of chitosan and the C=O and OH groups of Na-alginate. Peaks at 1691 cm^{-1} and 929 cm^{-1}, corresponding to C–O stretching and out-of-plane OH bending of lipoic acid, were reduced in intensity or disappeared, indicating interaction with chitosan and alginate. The carbonyl (C=O) band shifted from 1603 cm^{-1} in Na-alginate to 1616 cm^{-1} due to the presence of chitosan, while the Na–O peak of sodium alginate remained. A new peak at 1746 cm^{-1}, corresponding to the asymmetric stretching of the COO group, indicates interaction between the carboxyl group of alginate and the amino group of chitosan, likely forming amide linkages. The overall reduction in peak intensity and shifts in wavenumbers indicate improved dispersion of LA within the chitosan-alginate complex. These spectral changes suggest successful interactions between the components, such as alginate, chitosan, and lipoic acid, indicating the formation of a stable biopolymeric complex.

In the spectra of glutaraldehyde-crosslinked samples (Fig. 3B), the hydroxyl peak for crosslinker-free complexes appeared at 3431 cm^{-1} and shifted to a lower wavenumber of 3424 cm^{-1}. The intensity of the peak corresponding to the -COO stretching at 1746 cm^{-1} also showed a shift. In the spectra of MMT, peaks were observed at 3635 cm^{-1}, 1639 cm^{-1}, and in the range 1051-544 cm^{-1},corresponding to -OH stretching, -OH bending, and oxide bends of metals like Si, Al, and Mg.For the MMT-loaded samples, the peak at 1746 cm^{-1} in chitosan shifted to 1737 cm^{-1} for the complex. In the spectrum of the glutaraldehyde crosslinked lipoic acid-loaded chitosan-MMT-alginate system (Fig. 3C), the characteristic peaks of chitosan, alginate, MMT, and lipoic acid were present, although their intensities were reduced. These observations indicate enhanced MMT and lipoic acid dispersion within the chitosan-alginate complex.

X-ray diffraction study

LA exhibits distinct sharp peaks at 2θ = 23° and 2θ = 19°, which indicate its crystalline nature as in Fig. 4A. The diffractogram of the CA system showed a distinct broad peak at 2θ = 21°, with a minor right shift on the addition of crosslinker and MMT (Fig. 4B). The characteristic peaks for lipoic acid disappeared in the diffractogram of the drug-loaded complex. This suggests the formation of an

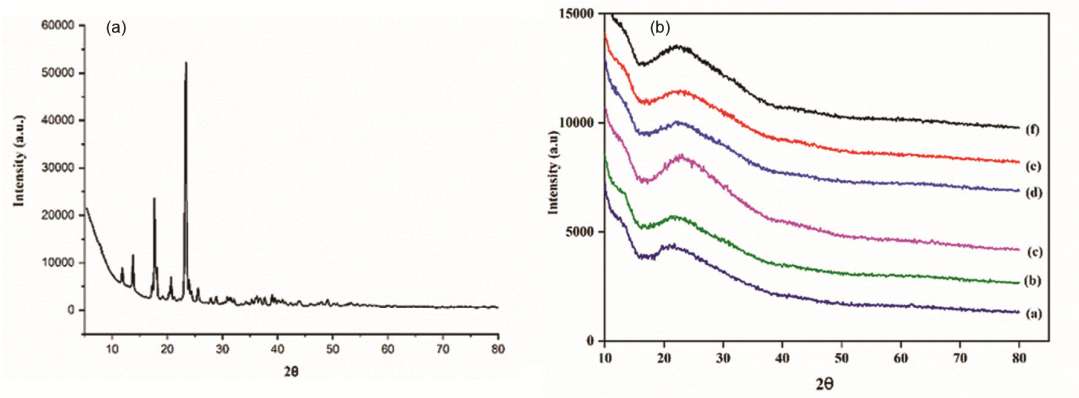

Fig. 4 — XRD patterns of (A) Lipoic acid and (B) (a) CA, (b) CA/GA1, (c) CA/GA3, (d) CA/M1, (e) CA/M3, (f) CA/GA2/M2

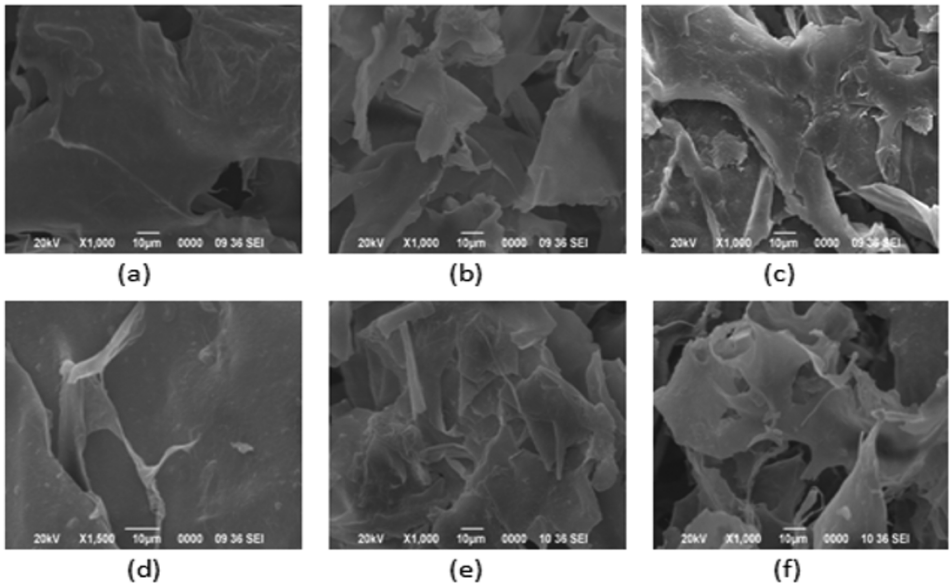

Fig. 5 — SEM micrographs of (a) CA, (b) CA/GA1, (c) CA/GA3, (d) CA/M1, (e) CA/M3, (f) CA/GA2/M2

amorphous region, likely due to the suppression of the drug's crystallisation within the confinement of the polymer matrix[49,50]. This also indicates the molecular-level dispersion of LA within the complex and the amorphous or disordered crystalline nature of LA in the polymer matrix. The transition to an amorphous state (as suggested by the disappearance of these peaks for drug-loaded formulations) can significantly enhance the drug's solubility and bioavailability[51].

Scanning electron microscope (SEM) study

SEM analysis examined the surface morphologies of drug-loaded polyelectrolyte complexes with varying concentrations of MMT and crosslinker (Fig. 5). The surface of CA appeared smooth. The surface smoothness decreased gradually with the increase in crosslinker concentration (Fig. 5b and 5c), indicating increased interaction between the CA complex and GA. An increase in the concentration of GA has resulted in densification, which can be seen in the SEM images (Fig. 5b, 5c, 5f). The inclusion of MMT (0.3%) (Fig. 5d) did not much change in surface morphology compared to the CA complex. However, a further increase in MMT (4.8%) (Fig. 5e) has resulted in a rougher, more textured surface, suggesting an agglomeration of MMT. The combined inclusion of MMT and GA produced a more uneven complex than the one without MMT and CA (Fig. 5f). These surface modifications indicate effective crosslinking and good interaction between MMT and the base polymer molecules[52,53].

The roughness in surface morphology can enhance the adhesion of drug delivery systems to the intestinal wall, which is beneficial for localised treatment. The

increased surface area allows for more effective interaction with the mucosal layer, leading to prolonged retention time in the intestine and improved therapeutic efficiency[54].

Glucose Uptake Assay

Insulin resistance is a key characteristic of type 2 diabetes mellitus. The insulin signalling pathway is activated when insulin attaches to its specific receptor on cells that respond to insulin, triggering a cascade of signals that promotes the movement of the GLUT4 glucose transporter from the cytoplasm to the cell surface, facilitating glucose entry into the cells[55]. It is well recognised that elevated circulating saturated free fatty acids, especially palmitate, disrupt insulin signalling and contribute to insulin resistance[56]. Given that skeletal muscle cells are responsible for over 70% of insulin-mediated glucose transport, we examined the impact of our LA-loaded PECs on averting palmitate-induced insulin resistance in skeletal muscle cells and the results are shown in Fig. 6. The formulations significantly mitigated the impairment of insulin-stimulated 2-NBDG uptake by L6 myotubes due to palmitate.The control group's glucose uptake was markedly lower than all treated groups, illustrating the basal glucose transport activity without stimulation. In contrast, the palmitic acid group served as a pathological control, showing decreased glucose uptake characteristic of lipid-induced insulin resistance. This reduction in glucose uptake is consistent with the deregulated metabolic state observed in type 2 diabetes, where lipid accumulation in muscle tissues impairs insulin signalling pathways.

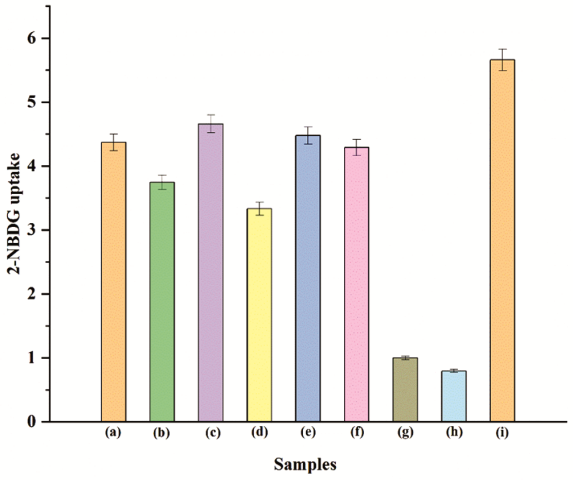

Fig. 6 — Glucose uptake assay performed for (a) CA/GA2/M2, (b) CA/M3, (c) CA/M1, (d) CA/GA3, (e) CA/GA1, (f) CA, (g) Control, (h) Palmitate and (i) Insulin

All of our samples significantly enhanced glucose uptake in the cells. The formulations could help lower blood glucose levels in circulation by promoting glucose uptake into peripheral cells. Samples containing 0.3% w/w MMT showed marginally higher glucose uptake than MMT-free CA. Glucose uptake was found to decrease with the increase in MMT concentration. The inclusion of MMT controlled the release of LA due to the presence of intricate silicate layers. A higher percentage of MMT incorporation hindered LA's release efficiently, reducing its glucose uptake effectiveness. Similarly, adding GA at a lower percentage didn't significantly improve the glucose uptake. Still, a higher concentration of GA incorporation reduced the glucose uptake due to the less availability of LA caused by the compact structure due to cross-linking. However, the combined addition of GA and MMT exhibited similar levels of glucose uptake. Consequently, these findings suggest the potential of developing lipoic acid-loaded systems as effective hypoglycaemic agents. CA/M1, CA/GA1, CA, and CA/GA2/M2 showed the best results. This comparatively better performance can be attributed to a combination of factors like better drug loading, better drug release, and the influence of the formulations on the vitality and metabolic activities of the cells[52,57]. These findings are consistent with previous studies that have demonstrated the efficacy of lipoic acid in improving insulin sensitivity and glucose uptake. For instance, Midaoui *et al*. reported that α-lipoic acid plays a role in preventing insulin resistance by enhancing glucose uptake in peripheral tissues[3]. Similarly, Lee *et al*. showed that Lipoic acid increases glucose uptake by activating AMP-activated protein kinase (AMPK) in skeletal muscle cells, thereby improving insulin sensitivity[5].

Cell Viability Assay

Cytotoxicity assay performed for the lipoic acid-loaded systems with varying concentrations of GA and MMT are shown in Fig. 7. The cell viability assays, conducted using the MTT method, demonstrated that all tested formulations exhibited excellent biocompatibility with no significant cytotoxicity observed across the tested concentrations. Cell viability studies indicated a dose-dependent response in cell lines treated with higher concentrations of MMT, specifically in samples such as CA/M3. This response was attributed to these formulations' reduced release of LA. Conversely,

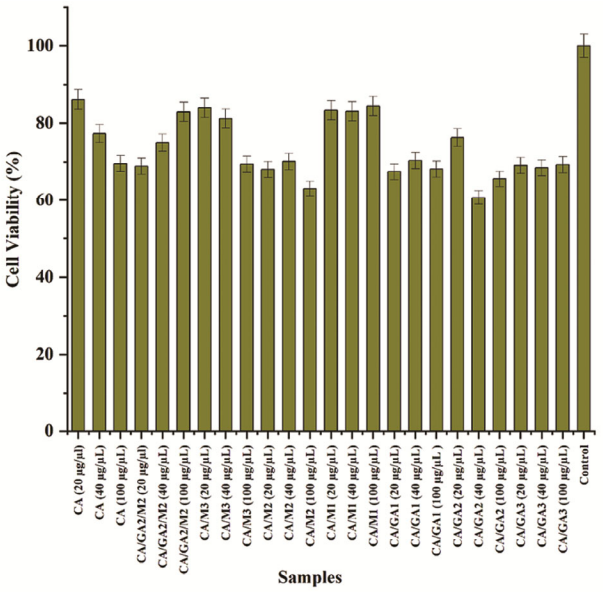

Fig. 7 — Cytotoxicity assay performed for the lipoic acid-loaded systems with varying concentrations of GA and MMT

samples containing a lower percentage of MMT (CA/M1) displayed the highest cell viability and did not exhibit a dose-dependent response. The silicate layers within MMT were instrumental in controlling LA release, influencing cell viability. Additionally, variations in the percentage of glutaraldehyde across the samples did not significantly impact cell viability, suggesting that differences in crosslinker concentration were not detrimental. The formulation containing both MMT and glutaraldehyde (CA/GA/M2) elicited a dose-dependent increase in cell viability in diabetic cell lines, likely due to the enhanced availability of LA. In contrast, formulations devoid of MMT or crosslinkers displayed slight cytotoxicity at higher doses, underscoring that cell viability depends on LA's availability, which is regulated by the amount of crosslinker present.

Our findings are consistent with previous studies highlighting the biocompatibility of chitosan and alginate-based drug delivery systems. For instance, Prabaharan and Mano reported that chitosan-based particles are well-tolerated in cellular systems due to their biodegradability and non-toxic nature[12]. Similarly, studies by Oliveira *et al*. confirmed that biopolymer films crosslinked with GA, when used at controlled concentrations, exhibit good biocompatibility without inducing significant cytotoxic effects[27].

George and Shrivastav observed that excessive GA crosslinking reduced cell viability in alginate-based hydrogels, potentially due to the formation of rigid polymer networks that hinder cell proliferation[24]. In contrast, our formulations with higher GA concentrations did not show significant cytotoxic effects. This is likely due to the optimised balance between crosslinker concentration and the biopolymer matrix, which preserved the formulations' overall structural flexibility and biocompatibility.

Moreover, our findings align with the research of Marapureddy and Thareja, who demonstrated that including nanofillers, such as MMT, can improve the mechanical strength of the delivery system without negatively impacting cell viability[25]. In our study, the incorporation of MMT at lower concentrations (e.g., CA/M1) improved cell viability, suggesting that moderate levels of MMT can enhance the mechanical properties of the formulations without compromising biocompatibility.

Overall, our study demonstrates that careful modulation of both GA and MMT concentrations can maintain or even enhance cell viability, reinforcing the potential of these formulations for future drug development. By optimising these parameters, we have successfully created a system that improves therapeutic efficacy and ensures cell safety, particularly in long-term treatments for chronic diseases such as type 2 diabetes.

Conclusion

This study successfully synthesised LA-loaded chitosan-alginate polyelectrolyte complexes, incorporating varying concentrations of GA and MMT as functional additives. Encapsulation efficiency was higher in formulations devoid of GA and MMT, indicating that these additives influence the entrapment of LA within the polymer matrix. FTIR spectroscopy confirmed the successful loading of LA through observable shifts and reductions in characteristic peaks corresponding to chitosan, alginate, MMT, and LA, suggesting strong interactions between the drug and the polymeric components. XRD analysis revealed the suppression of LA's crystallinity, indicating that the drug was present in an amorphous state within the polymer matrix. This transition enhances the solubility and bioavailability of LA. SEM images depicted complex with dense, rough surfaces, indicating the interaction between the polymer network and the drug. Drug release studies demonstrated that the formulation exhibited pH-dependent release, with increased release observed in alkaline conditions, aligning with the intended controlled release profile. Furthermore,

higher GA concentrations reduced the drug release due to increased crosslinking density, which restricted polymer swelling and drug diffusion. Similarly, increasing MMT content decreased cumulative drug release. All formulations significantly enhanced glucose uptake in glucose uptake studies and showed good cell viability. These findings highlight the potential of these LA-loaded chitosan-alginate complexes as effective drug delivery systems.

References

1 Zhang P, Zhang X, Brown J, Vistisen D, Sicree R, Shaw J & Nichols G, Global healthcare expenditure on diabetes for 2010 and 2030, *Diabetes Res Clin Pract*, 87 (2010) 293.

2 Shaw J E, Sicree R A & Zimmet P Z, Global estimates of the prevalence of diabetes for 2010 and 2030, *Diabetes Res Clin Pract*, 87 (2010) 4.

3 Midaoui A E L & de Champlain J, Prevention of hypertension, insulin resistance, and oxidative stress by α-Lipoic acid, *Hypertension*, 39 (2002) 303.

4 Kandeil M A, Amin K A, Hassanin K A, Ali K M & Mohammed E T, Role of lipoic acid on insulin resistance and leptin in experimentally diabetic rats, *J Diabetes Complicat*, 25 (2011) 31.

5 Lee W J, Song K H, Koh E H, Won J C, Kim H S, Park H S, Kim M S, Kim S W, Lee K U & Park J Y, α-Lipoic acid increases insulin sensitivity by activating AMPK in skeletal muscle, *Biochem Biophys Res Commun*, 332 (2005) 885.

6 Tripathi A K, Ray A K, Mishra S K, Bishen S M, Mishra H & Khurana A, Molecular and therapeutic insights of alpha-lipoic acid as a potential molecule for disease prevention, *Revista Brasileira de Farmacognosia*, 33 (2023) 272.

7 Diesel B, Kulhanek-Heinze S, Höltje M, Brandt B, Höltje H D, Vollmar A M & Kiemer A K, α-Lipoic acid as a directly binding activator of the insulin receptor: Protection from hepatocyte apoptosis, *Biochemistry*, 46 (2007) 2146.

8 Capece U, Moffa S, Improta I, Di-Giuseppe G, Nista E C, Cefalo C M A, Cinti F, Pontecorvi A, Gasbarrini A, Giaccari A & Mezza T, Alpha-lipoic acid and glucose metabolism: A comprehensive update on biochemical and therapeutic features, *Nutrients*, 15 (2022) 18.

9 Salehi B, Berkay Y Y, Antika G, Boyunegmez T T, Fawzi M M, Lobine D, Akram M, Riaz M, Capanoglu E, Sharopov F, Martins N, Cho W C & Sharifi-Rad J, Insights on the use of α-Lipoic acid for therapeutic purposes, *Biomolecules*, 9 (2019) 356.

10 Das A, Ringu T, Ghosh S & Pramanik N, A comprehensive review on recent advances in preparation, physicochemical characterization, and bioengineering applications of biopolymers, *Polym Bullet*, 80 (2023) 7247.

11 Jabeen N & Atif M, Polysaccharides based biopolymers for biomedical applications: A Review, *Polym Adv Technol*, 35 (2024) e6203.

12 Prabaharan M & Mano J F, Chitosan-based particles as controlled drug delivery systems, *Drug Deliv*, 12 (2004) 41.

13 Nasef S M, Khozemy E E & Mahmoud G A, pH-responsive chitosan/acrylamide/gold/nanocomposite supported with silver nanoparticles for controlled release of anticancer drug, *Sci Rep*, 13 (2023) 7818.

14 Azmana M, Mahmood S, Hilles A R, Rahman A, Arifin M A & Bin A S, A review on chitosan and chitosan-based bionanocomposites: Promising material for combatting global issues and its applications, *Int J Biol Macromol*, 185 (2021) 832.

15 Dilruba-Öznur K G & Ayşe-Pınar T D, Statistical evaluation of biocompatibility and biodegradability of chitosan/gelatin hydrogels for wound-dressing applications, *Polym Bullet*, 81 (2024) 1563.

16 Lima D S, Tenório-Neto E T, Lima-Tenório M K, Guilherme M R, Scariot D B, Nakamura C V, Muniz E C & Rubira A F, pH-responsive alginate-based hydrogels for protein delivery, *J Mol Liq*, 262 (2018) 29.

17 Hariyadi D M & Islam N, Current status of alginate in drug delivery, *Adv Pharmacol Pharm Sci*, 2020 (2020) 1.

18 Abourehab M A S, Rajendran R R, Singh A, Pramanik S, Shrivastav P, Ansari M J, Manne R, Amaral L S & Deepak A, Alginate as a promising biopolymer in drug delivery and wound healing: A review of the state-of-the-art. *Int J Mol Sci*, 23 (2022) 9035.

19 Sipos B, Benei M, Katona G & Csóka I, Optimization and characterization of sodium alginate beads providing extended release for antidiabetic drugs, *Molecules*, 28 (2023) 6980.

20 Pan C T, Chien S T, Chiang T C, Yen C K, Wang S Y, Wen Z H, Yu C Y & Shiue Y L, Optimization of the spherical integrity for sustained-release alginate microcarriers-encapsulated doxorubicin by the taguchi method, *Sci Rep*, 10 (2020) 21758.

21 Sen O, Manna S, Nand G, Jana S & Jana S, Recent advances in alginate based gastroretentive technologies for drug delivery applications, *Med Nov Technol Devices*, 18 (2023) 100236.

22 Ramdhan T, Ching S H, Prakash S & Bhandari B, Physical and mechanical properties of alginate based composite gels, *Trends Food Sci Technol*, 106 (2020) 150.

23 Wang F, Li L, Zhu X, Chen F & Han X, development of pH-responsive polypills via semi-solid extrusion 3d printing, *Bioengineering*, 10 (2023) 402.

24 George A & Shrivastav P S, Preparation and evaluation of chitosan-alginate/carrageenan hydrogel for oral drug delivery in the treatment of diabetes, *J Bioact Compat Polym*, 38 (2023) 368.

25 Marapureddy S G & Thareja P, Synergistic effect of chemical crosslinking and addition of graphene-oxide in chitosan-hydrogels, films, and drug delivery, *Mater Today Commun*, 31 (2022) 103430.

26 Pakolpakçil A, Effect of glutaraldehyde crosslinking parameters on mechanical and wetting properties of PVA/ NaAlg electrospun mat, *Sakarya Univ J Sci*, 26 (2022) 990.

27 Oliveira A C S, Ugucioni J C & Borges S V, Effect of glutaraldehyde/glycerol ratios on the properties of chitosan films, *J Food Process Preserv*, 45 (2021) 15060.

28 ul-Haque S & Nasar A, Inamuddin montmorillonite clay nanocomposites for drug delivery, *Appl Nanocompos Mater Drug Deliv*, *Elsevier*, (2018) 633.

29 Katti K S, Jasuja H, Jaswandkar S V, Mohanty S & Katti D R, Nanoclays in medicine: A new frontier of an ancient medical practice, *Mater Adv*, 3 (2022) 7484.

30 Uddin M N, Hossain M T, Mahmud N, Alam S, Jobaer M, Mahedi S I & Ali A, Research and applications of nanoclays: A review, *SPE Polym*, 5 (2024) 507.

31 Jayrajsinh S, Shankar G, Agrawal Y K & Bakre L, Montmorillonite nanoclay as a multifaceted drug-delivery carrier: A review, *J Drug Deliv Sci Technol*, 39 (2017) 200.

32 Gogoi P, Dutta A, Ramteke A & Maji T K, Preparation, characterization and cytotoxic applications of curcumin-(±) <scp>α-lipoic</Scp> acid coloaded phosphorylated chitosan nanoparticles in <scp>MDA MB</Scp> 231 breast cancer cell line, *Polym Adv Technol*, 31 (2020) 2827.

33 Banik N, Hussain A, Ramteke A, Sharma H K & Maji T K, Preparation and evaluation of the effect of particle size on the properties of chitosan-montmorillonite nanoparticles loaded with isoniazid, *RSC Adv*, 2 (2012) 10519.

34 Devi N & Maji T K, Microencapsulation of isoniazid in genipin-crosslinked gelatin-A–κ-carrageenan polyelectrolyte complex, *Drug Dev Ind Pharm*, 36 (2010) 56.

35 Gogoi P, Das M K, Ramteke A & Maji T K, Soy flour–ZnO nanoparticles for controlled release of silibinin: Effect of ZnO nanoparticle, surfactant, and cross-linker, *Int J Polym Mater Polym Biomater*, 67 (2018) 543.

36 Devi N & Maji T K, Preparation and evaluation of gelatin/ sodium carboxymethyl cellulose polyelectrolyte complex microparticles for controlled delivery of isoniazid, *AAPS Pharm Sci Tech*, 10 (2009) 1412.

37 Cassano R, Trombino S, Ferrarelli T, Mauro M V, Giraldi C, Manconi M, Fadda A M & Picci N, Respirable rifampicin-based microspheres containing isoniazid for tuberculosis treatment, *J Biomed Mater Res*, 100A (2012) 536.

38 Tan J M, Karthivashan G, Arulselvan P, Fakurazi S & Hussein M Z, Characterization and *In Vitro* sustained release of silibinin from pH responsive carbon nanotube-based drug delivery system, *J Nanomater*, 2014 (2014) 439873.

39 Pal D, Dasgupta S, Kundu R, Maitra S, Das G, Mukhopadhyay S, Ray S, Majumdar S S & Bhattacharya S, Fetuin-A acts as an endogenous ligand of TLR4 to promote lipid-induced insulin resistance, *Nat Med*, 18 (2012) 1279.

40 Mazumder S, Sinha A, Ghosh S, Sharma G C, Prusty B M, Manna D, Pal D, Pal C & Dasgupta S, *Leishmania* LPG interacts with LRR5/LRR6 of macrophage TLR4 for parasite invasion and impairs the macrophage functions, *Pathog Dis*, 81 (2023) 19.

41 Kumar P, Nagarajan A & Uchil P D, Analysis of cell viability by the MTT assaym, *Cold Spring Harb Protoc*, 2018 (2018) 095505.

42 Yuan Y, Chesnutt B M, Utturkar G, Haggard W O, Yang Y, Ong J L & Bumgardner J D, The effect of cross-linking of chitosan microspheres with genipin on protein release, *Carbohydr Polym*, 68 (2007) 561.

43 Hua S, Yang H & Wang A, A pH-sensitive nanocomposite microsphere based on chitosan and montmorillonite with in vitro reduction of the burst release effect, *Drug Dev Ind Pharm*, 36 (2010) 1106.

44 Assaad E, Wang Y J, Zhu X X & Mateescu M A, Polyelectrolyte complex of carboxymethyl starch and chitosan as drug carrier for oral administration, *Carbohydr Polym*, 84 (2011) 1399.

45 Sağlam D, Venema P, de Vries R & van der Linden E, The influence of pH and ionic strength on the swelling of dense protein particles, *Soft Matter*, 9 (2013) 4598.

46 Iman M & Maji T K, Effect of crosslinker and nanoclay on starch and jute fabric based green nanocomposites, *Carbohydr Polym*, 89 (2012) 290.

47 Nastaj J, Przewłocka A & Rajkowska-Myśliwiec M, Biosorption of Ni(II), Pb(II) and Zn(II) on calcium alginate beads: equilibrium, kinetic and mechanism studies, *Polish J Chem Technol*, 18 (2016) 81.

48 Ikuta N, Tanaka A, Otsubo A, Ogawa N, Yamamoto H, Mizukami T, Arai S, Okuno M, Terao K & Matsugo S, Spectroscopic studies of R(+)-α-Lipoic acid-cyclodextrin complexes, *Int J Mol Sci*, 15 (2014) 20469.

49 Maeda H, Onodera T & Nakayama H, Inclusion complex of α-Lipoic acid and modified cyclodextrins, *J Incl Phenom Macrocycl Chem*, 68 (2010) 201.

50 Yallapu M M, Gupta B K, Jaggi M & Chauhan S C, Fabrication of curcumin encapsulated PLGA nanoparticles for improved therapeutic effects in metastatic cancer cells, *J Colloid Interface Sci*, 351 (2010) 19.

51 Schittny A, Huwyler J & Puchkov M, Mechanisms of increased bioavailability through amorphous solid dispersions: A review, *Drug Deliv*, 27 (2020) 110.

52 Dong Y & Feng S S, Poly(d,l-Lactide-Co-Glycolide)/ montmorillonite nanoparticles for oral delivery of anticancer drugs, *Biomaterials*, 26 (2005) 6068.

53 Cai X, Riedl B, Zhang S Y & Wan H, The impact of the nature of nanofillers on the performance of wood polymer nanocomposites, *Compos Part A Appl Sci Manuf*, 39 (2008) 727.

54 Jawadi Z, Yang C, Haidar Z S, Santa-Maria P L & Massa S, Bio-inspired muco-adhesive polymers for drug delivery applications, *Polymers*, 14 (2022) 5459.

55 Saltiel A R & Kahn C R, Insulin signalling and the regulation of glucose and lipid metabolism, *Nature*, 414 (2001) 799.

56 Roden M, Price T B, Perseghin G, Petersen K F, Rothman D L, Cline G W & Shulman G I, Mechanism of free fatty acid-induced insulin resistance in humans, *J Clin Investig*, 97 (1996) 2859.

57 Abay A, Simionato G, Chachanidze R, Bogdanova A, Hertz L, Bianchi P, van den Akker E, von Lindern M, Leonetti M, Minetti G, Wagner C & Kaestner L, Glutaraldehyde-A subtle tool in the investigation of healthy and pathologic red blood cells, *Front Physiol*, 10 (2019) 00514.